Arab J Geosci (2015) 8:2121–2130
DOI 10.1007/s12517-014-1278-1

ORIGINAL PAPER

Analyses of the Persian Gulf sea surface temperature: prediction and detection of climate change signals

A. Shirvani · S. M. J. Nazemosadat · E. Kahya

Received: 14 October 2013 / Accepted: 3 January 2014 / Published online: 17 January 2014

Abstract This study was motivated by two main concerns including (a) prediction of the Persian Gulf Sea surface temperature (PGSST) anomalies using an autoregressive integrated moving average (ARIMA) model and (b) detection of the climate change signatures in the considered SST data. An ARIMA model was, therefore, developed to predict the SST anomalies having lead times from 1 to 3 months. While the SST time series for the period of 1950–2006 used to fit the model, corresponding records for January 2007 to June 2011 were applied as the test data. The developed model had a minimum value of Akaike information criterion, and its parameters were significantly different from zero. The correlation coefficients between the observed and simulated data for the lead times of 1, 2, and 3 months were found to be significant and equal to 0.72, 0.69, and 0.65, respectively. The corresponding hit rates were estimated as 79, 75, and 72 %, indicating a reasonable forecasting capability of the model. The Heidke's forecast scores were 0.59, 0.52, and 0.48 for the prediction schemes having 1, 2, and 3 months of lead time, respectively. It is shown that the Persian Gulf skin temperatures have warmed up about 0.57 °C during the 732 successive months of the period 1950–2010 noted as an upward significant trend. Although a significant trend was not evident for the 1950–1969 and 1970–1989 period, the PGSST has abruptly increased during the recent two decades. Almost all of the observed warming in the PGSST data is related to this period.

A. Shirvani (✉) · S. M. J. Nazemosadat
Department of Water Engineering and the Oceanic and Atmospheric Research Center, College of Agriculture, Shiraz University, Shiraz, Iran
e-mail: am_shirvani@hotmail.com

E. Kahya
Department of Civil Engineering, Istanbul Technical University, Istanbul, Turkey

Keywords Persian Gulf · Sea surface temperature · Prediction · ARIMA model · Climate change · Indian Ocean

Introduction

The Persian Gulf (Fig. 1) Sea surface temperature (PGSST) plays an influential role in precipitation variability over most parts of Iran and particularly its southwestern districts. Previous studies indicated that the above normal winter precipitation in southern Iran generally coincides with the periods that the SSTs are below their climatological mean (Nazemosadat 1998). On the other hand, the frequency of wintertime droughts generally corresponds to the spells that SSTs are above normal. Nazemosadat and Shirvani (2006) used the canonical correlation analysis (CCA) to assess the potential of PGSST data as the precipitation predictor in southwestern Iran. According to their reports, the first four empirical orthogonal functions of these SSTs accounted for about 27 % of total variance in winter precipitation of the study areas. Nazemosadat et al. (2008) analyzed the couple effects of the PGSST and the El Niño Southern Oscillation on rainfall variability in western and northwestern parts of Iran. They have shown that during the El Niño years, positive/negative anomalies of the PGSSTs generally coincided with above/below normal winter precipitation over the study area. For the La Niña episodes, however, wet or dry events are expected for these regions if the PGSSTs are colder or warmer than usual, respectively. In other words, wet or dry wintertime is expected for western and northwestern parts of Iran when the PGSST anomalies are in-phase or out-phase with the corresponding anomalies over equatorial parts of the eastern Pacific Ocean. Kämpf and Sadrinasab (2006) employed a three-dimensional hydrodynamic model to study the circulation and water mass properties of the Persian Gulf.

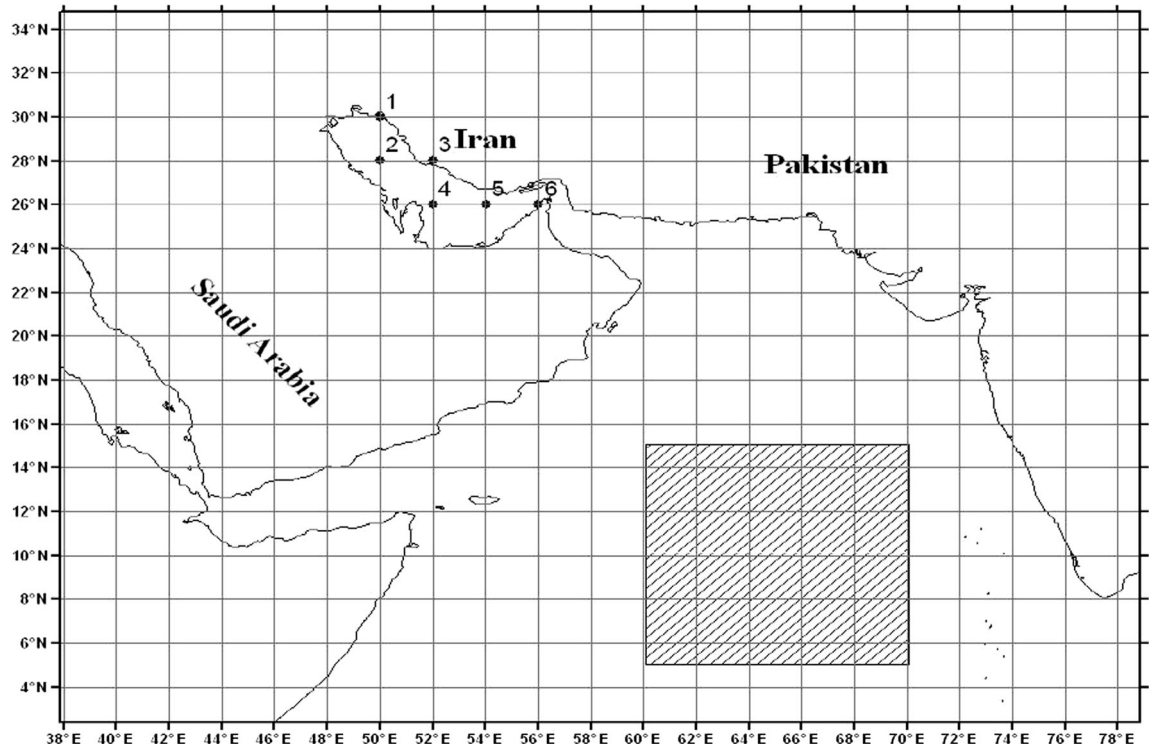

Fig. 1 The geographical location of the used grids in the Persian Gulf and northern parts of the Indian Ocean

They reported that the this water body experiences a distinct seasonal cycle in which a Gulf-wide cyclonic overturning circulation establishes in spring and summer, but this disintegrates into mesoscale eddies in autumn and winter. Johns et al. (2003) studied the water exchange between the Persian Gulf and the Indian Ocean through the Strait of Hormuz.

Yao and Johns (2010) studied the circulation and water mass transformation processes in the Persian Gulf and the water exchange with the Indian Ocean through the Strait of Hormuz using the Hybrid Coordinate Ocean Model. Their results suggest that the intruded Indian Ocean surface water is transformed into hypersaline waters with salinity >41 practical salinity unit by the fresh water loss in the northern end of the Gulf and in the southern shallow banks. Bauman et al. (2012) examined the size structure of four locally abundant corals in two regions of the Persian Gulf: the southern Gulf (Dubai and Abu Dhabi) and eastern Gulf (western Musandam). They reported that all corals in the southern Gulf were significantly smaller, and their size structure positively skewed and relatively more leptokurtic (i.e., peaky) compared to corals in the eastern Gulf. They have indicated that sea surface temperature, salinity, and the recent frequency of mass bleaching are all higher in the southern Gulf, suggesting higher mortality rates and/or slower growth in these populations. Copsey et al. (2006) presented strong evidence that the Indian Ocean warming was associated with local increases in sea level pressure during the period 1950–1996.

A variety of mathematical and statistical approaches are applied to forecast the tropical SST data. Among the commonly used techniques are CCA (e.g., Barnston and Ropelewski 1992; Landman and Mason 2001), hybrid coupled modeling (e.g., Neelin 1990; Syu et al. 1995), linear inverse modeling (Penland and Magorian 1993; Penland and Matrosova 1999), Markov modeling (Xue et al. 2000), ensemble techniques (Krishnamurti et al. 2006), and neural networks (Martinez and Hsieh 2009). The outcome of such studies is routinely used for operational forecasting of the global tropics SST by the Physical Sciences Division, Earth Physical Laboratory, and National Oceanic and Atmospheric Administration (NOAA) at http://www.esrl.noaa.gov/psd/forecasts/seasonal/. In spite of such attention to equatorial regions, less consideration is given to the prediction of extratropical SSTs and particularly local water bodies such as the Persian Gulf.

Although autoregressive integrated moving average (ARIMA) models have been widely used in various scientific and engineering applications, to the best of our knowledge, not much research has been done applying such models for the prediction of SST behavior over tropical or extratropical ocean waters. Chu and Kats (1985, 1987) identified an ARIMA model for the prediction of monthly and seasonal values of the Southern Oscillation Index (SOI). Baker-Austin et al. (2012) have recently used ARIMA model to project the SST data for the Baltic Sea up to year 2050. Mazaris et al. (2004) developed some ARIMA and regression models to forecast variations in the breeding activity of loggerheads at

the Zakynthos Island, West Greece. In general, the ARIMA processes have several advantages over other methods including its capability to simulate the path of forecasting, its rich information on time-related changes, and the consideration of serial correlation between observations.

In addition to forecasting, analyzing the SST time series is also critically important for the detection and modeling of climate change. The trend in global SST is one of the primary physical impacts of climate change that affects the interactions between ocean, atmosphere, and land in global and local scales. On the basis of Baker-Austin et al. report (2012), the observed warming patterns in the Baltic Sea SSTs coincided with the unexpected emergence of *Vibrio* infections in northern Europe. Nazemosadat et al. (2006) detected the climate change signal in Iran's precipitation that was consistent with the change in SOI data for the period 1951–1999. According to their findings, the mid-1970s is the most probable change-point year for these two distinct datasets.

The aim of the present study is to develop an ARIMA model for the prediction of SST anomalies over the Persian Gulf. Furthermore, detecting significant trend in the monthly SST data is the other goal of the study. The study has also endeavored to differentiate the natural and anthropogenic signals of climate change over the Persian Gulf.

SST data

Monthly SST anomalies of six 2°×2° resolution grid points in the Persian Gulf (Fig. 1) as well as for 25 grid points in tropical parts of the Indian Ocean (IO: 60°E to 70°E; 5°N to 15°N) were gratefully obtained from the NOAA Improved Extended Reconstructed SST version 3 (ERSST.v3) database for the period 1951–2011 (Smith et al. 2008). This database has already been bias-adjusted for the period after 1985 using the satellite-based infrared data collected from the advanced very high resolution radiometer (AVHRR). The dataset is available online at http://www.esrl.noaa.gov/psd/data/gridded/data.noaa.ersst.html.

The obtained anomalies were firstly weighted according to cosine value of their associated grids. The anomalies are computed with respect to 1971–2000 month climatology as described by Xue et al. (2003). The average values of these anomalies (for the prescribed 6 and 25 grids) were then computed and used as the Persian Gulf and the Indian Ocean SSTs, respectively. The SST data over the Indian Ocean tropics were used for comparison with the Persian Gulf SSTs as will be discussed later.

For assessing the reliability of the applied SST data (ERSST.v3) and for consolidating our results, the study has also simultaneously analyzed another high temporal (1 day) and spatial (0.25°×0.25° grids) resolutions of the satellite-based SST dataset (Martin et al. 2012; Reynolds et al. 2007). The Optimum Interpolated version of this SST product (namely, level 4 of OISST) which is available for the periods after 20 September 1981 was extracted from http://www.ncdc.noaa.gov/oa/climate/research/sst/oi-daily-information.php webpage. For making these high resolution data compatible with the ERSST.v3 SSTs, the OISSTs records were averaged in time and space to produce the monthly 2°×2° SST time series. Difference between the monthly values of these two datasets as well as between their associated ARIMA models was then investigated.

For model development, the applied anomaly series were divided into two sets of records consisting of January 1950 to December 2006 (684 months) and January 2007 to June 2011 (54 months). While the first dataset was used for developing the proposed ARIMA model, the later one was applied for model verification.

For detecting the climate change signals, characteristics of the SST-time regressions were examined for the whole record length of the study period (1950 to mid-2011, 738 months). These regressions were applied for both the Persian Gulf and Indian Ocean datasets. Furthermore, the considered 738 months were divided into 240, 240, and 252 successive months (1950–1969, 1970–1989, and 1990–2010, respectively) and their trend lines were captured and compared. The Indian Ocean dataset was assumed to be an unimpaired dataset that is affected by natural rather than anthropogenic sources of climate change. Therefore, comparison between climate change signals of this dataset with corresponding records of the Persian Gulf was considered as an alternative way for differentiating between the natural and anthropogenic sources of climate over the Persian Gulf.

Methods

ARMA versus ARIMA

Autoregressive (AR) and moving average (MA) models can effectively be coupled to form a general and useful class of time series called autoregressive moving average (ARMA) models. In an ARMA model, the current value of the time series is expressed as a linear aggregate of p previous values and a weighted sum of q previous deviations (original value minus fitted value of previous data) plus a random parameter.

Since ARMA models prefer stationary datasets as an input file, a differencing procedure is generally considered as a smart approach for transforming nonstationary series into the stationary series (Box and Jenkins 1976). In this case, instead of ARMA, the ARIMA models are used. Box and Jenkins (1976) popularized ARIMA models as ARIMA(p, d, q), where

p and q are the orders for nonseasonal AR and MA, respectively. The nonseasonal differencing parameter that shows how many differencing steps used for making the series stationary is shown by d. The general format of the ARIMA model is:

$$\phi_p(B)\nabla^d x_t = \theta_q(B)w_t \tag{3.1}$$

Where w_t is the white noise random variable. The ordinary autoregressive and moving average components are, respectively, represented by:

$$\phi_p(B) = 1-\varphi_1 B - \phi_2 B^2 - \ldots + \phi_p B^p, \tag{3.2}$$

And

$$\theta_q(B) = 1 + \theta_1 B + \theta_2 B^2 + \ldots + \theta_q B^q, \tag{3.3}$$

The ordinary difference component is defined by $\nabla^d=(1-B)^d$, where B is the backshift operator defined by $B^d x_t=x_{t-d}$.

Model development

Developing an ARIMA model consists of three stages including model identification, parameter estimation, and diagnostic checking (Box et al. 1994). For a given time series, these three stages are repeated until an optimized model is identified. In the first step, some initial models, which seem to represent the time series behavior and are worthy of parameter estimation, are identified (Box et al. 1994; Shumway and Stoffer 2006). This identification is essentially based on the characteristics of both autocorrelation and partial autocorrelation functions (ACF and PACF, respectively). Since these functions are practically unknown, they have to be estimated in order to identify a tentative model fitted to the observed series. In other words, the goal of model identification is coupling the unknown patterns in the sample ACF and PACF models with the already known of these two patterns in ARIMA models.

After the model was identified, parameter estimation needed to be considered. The model parameters should satisfy two conditions, namely stationarity and invertibility for the AR and MA parameters, respectively. Furthermore, relevant statistical tests should be considered to investigate if the estimated parameters are significantly different from zero. The values of standard error of estimation are also important and need to be assessed. As the parameters were estimated, the model adequacy was examined by checking whether w_t (in equation 3.1) is a white noise random variable with zero mean and constant variance. We therefore used the ACF analysis to check if the estimated residual series $(\widehat{w}_t)$ are white noise and do not exhibit any sign of nonrandomness.

Another useful statistical test which examines if the residuals are independent is the Box and Pierce (1970) or Ljung and Box (1987) test which is denoted by Q in the following equation.

$$Q = n(n+2)\sum_{h=0}^{H} \frac{\widehat{\rho}_e^2(h)}{n-h}, \tag{3.4}$$

Where $\widehat{\rho}_e(h)$ is the estimated autocorrelation coefficient of the residuals and n is the sample size. Ljung and Box (1987) showed that under the null hypothesis of model adequacy, Q statistic generally follows a $\chi^2_{(H-p-q)}$ distribution. Thus, one would reject the null hypothesis at level α if the value of Q exceeds the $(1-\alpha)$ quantile of the $\chi^2_{(H-p-q)}$ distribution.

In addition to the mentioned tests, we examined model adequacy by using the Akaike's information criterion (AIC) as introduced by Akaike (1974). The bias corrected from of AIC suggested by Sugiura (1987) is defined as

$$\mathrm{AICc} = \ln \widehat{\sigma}_k^2 + \frac{n+k}{n-k-2} \tag{3.5}$$

Where $\widehat{\sigma}_k^2$ is the variance of residuals in sample data and k is the number of model's parameters. Among various values of k, that statistic which yields minimum amount of AICc signifies the best model.

Detection of climate change

As indicated earlier, for each of the constructed time series with 732, 240, or 252 records, the SST-time regression was performed. In other words, linear trends of the SST series were computed for 1950–2011, 1950–1969, 1970–1989, and 1990–2010 periods. In addition to the whole Persian Gulf, we also examined the climate change signals for the northern and southern parts of the Gulf separately. While the average values of SST in grids 1, 2, and 3 made up the time series for the northern part of the Gulf, corresponding values for grids 4, 5, and 6 were considered as the SST data for southern parts of this water body (Fig. 1).

In addition to the Persian Gulf region, similar time-SST regression was also performed for another SST dataset which is obtained by averaging the 2°×2° SST data over a selected part of the eastern Indian Ocean tropics bounded between 60 and 70°E and between 5 and 15 N. This tropical part of the Ocean is located in the southeastern side of the Persian Gulf and is far from the continental coastlines and isolated from the anthropogenic signals of climate change. Comparison of the trend lines of historical SST data between these two distinct regions is considered as a reasonable approach for differentiating the

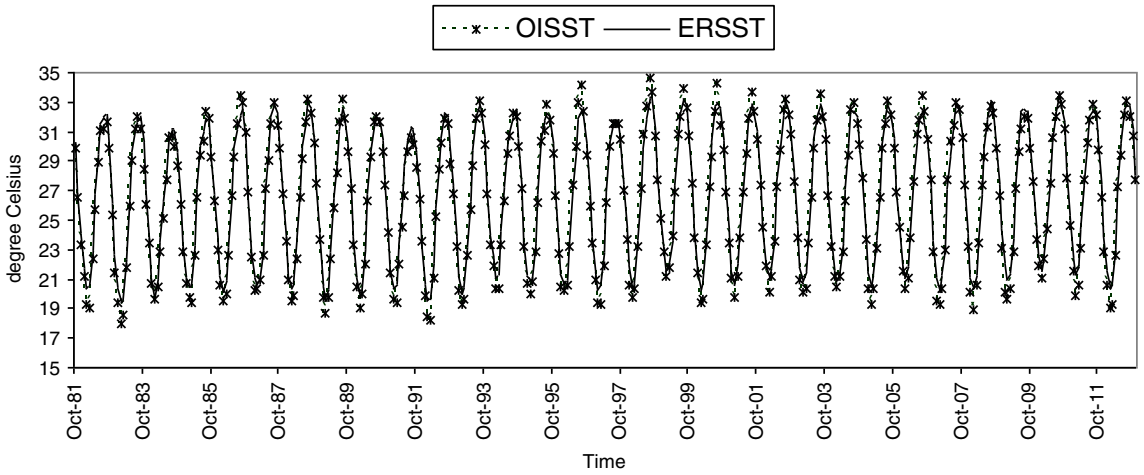

Fig. 2 The time series plot of ERSST (*solid*) and OISST (*dash*) for the Persian Gulf

anthropogenic and natural sources of climate change over the Persian Gulf.

Results

Ground-based versus satellite-based SSTs

The difference between historical values of ERSST.v3 and OISST AVHRR datasets (ERSST.v3–OISST) was calculated for the considered grid points over the Persian Gulf and Indian Ocean tropics (Fig. 2). The difference values were equal to 1.2, 0.19, 0.77, 0.25, −0.11, and 0.20 °C for grids 1, 2, 3, 4, 5, and 6 of the Persian Gulf, respectively (Fig 1). The difference was, however, generally smaller for the Indian Ocean SSTs. For instance, the subtraction result was equal to 0.22 °C for the grid located at 66°E and10°N. According to these statistics, for both of the study areas, the ground-based data are consistently greater than corresponding satellite-based series. Furthermore, differences are higher for the coastal regions and drop to its minimum values over the central parts of the considered water bodies.

Prediction of the PGSST data

The time series of the PGSST anomalies, say $pgsst_t$, from January 1950 to December 2006 was used for model development (Fig. 3). Since the ERSST.v3 dataset contained a longer record length, the ARIMA model was basically developed according to this dataset. The outputs were then compared with the similar models that were developed based on both ERSST.v3 and OISST for the periods after 1981. Results of this comparison revealed that the model structure and its associated orders are identical for all of the used datasets. Model coefficients were, however, found to be sensitive to the record length and the data acquisition methods.

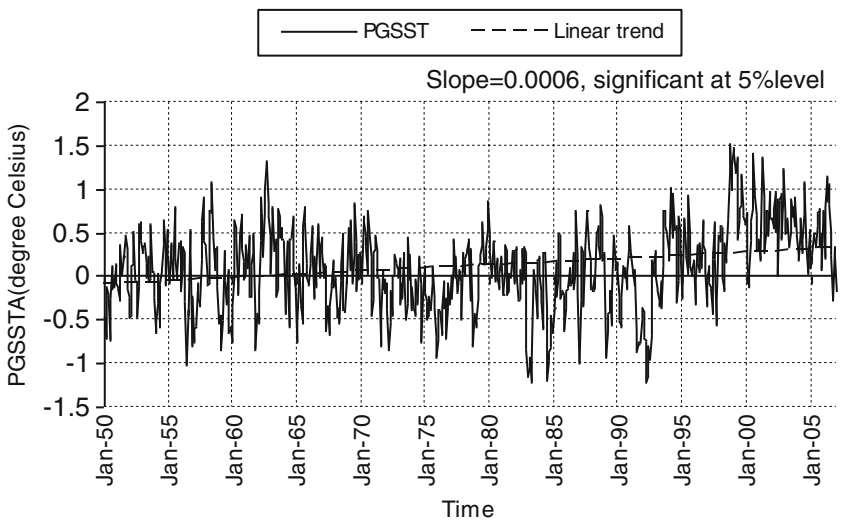

Fig. 3 Time series plot of PGSST anomalies for 1950–2006

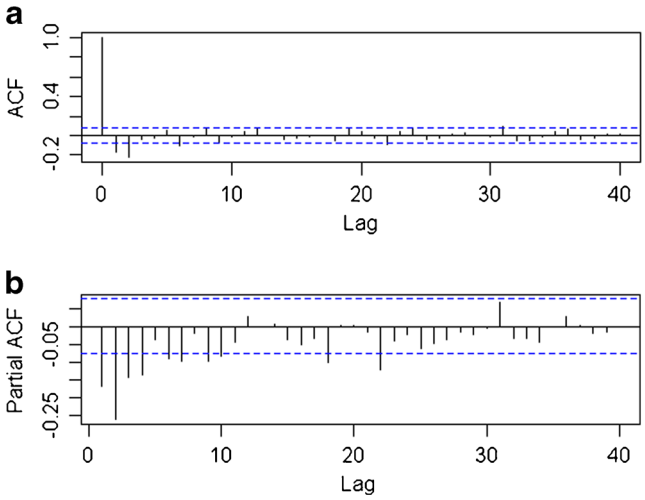

Fig. 4 **a** Sample autocorrelation function and **b** sample partial autocorrelation function of the differenced Persian Gulf sea surface temperature anomalies time series. The *dashed lines* indicate the interval of $\pm\frac{1.96}{\sqrt{n}}$

The herein presented discussion and results are, therefore, related to the ERSST.v3 dataset which started since 1950. The applied simple linear regression analysis revealed a significant (at 95 % level) upward trend in this dataset as follows:

$$\text{pgsst}_t = \beta_1 t + \beta_0 + w_t, \quad t = 1, 2, \ldots, 684,$$

Where w_t is the white noise random variable and t is the time in months starting at January 1950. The estimated slope $\widehat{\beta}_1$ was equal to 0.000605 °C/month, with standard error of 8.9×10^{-5}°C/month, indicating the existence of a significant warming trend in the applied time series. The Gulf SST has, therefore, increased by about 0.4°C for the period 1950–2006. Due to this significant upward trend, a first order differencing procedure (d=1) was performed to de-trend the dataset. The ACF analysis of the differenced series showed significant correlations at lags 1 and 2 (Fig. 4a) suggesting that the moving average model has two or less parameters (i.e., $q\leq2$). Since the plot of partial autocorrelation function exhibited significant correlations for the lags less than 5, an AR model with order 4 was suggested. After order identification, equations 3.2 and 3.3 were used to estimate the parameter values. The significance values of these parameters were eventually examined using the t test.

Among the candidate models, the most appropriate one which has minimum value of AICc was identified as the best choice. The selected optimal model which has ARIMA (1, 1, 2) structure and error variance of $\widehat{\sigma}_w^2 = 0.115$ is:

$$\left(1-0.48_{(0.087)}B\right)\nabla^1\text{pgsst}_t = \left(1-0.82_{(0.097)}B-0.13_{(0.080)}B^2\right)w_t \quad (4.1)$$

The given values in the parentheses signify the parameters' standard errors of estimate. All the presented coefficients were found to be statistically significant. For example, the t value of 0.48/0.087=5.5 is significantly greater than the quantile of t distribution with α=0.05 and 680° of freedom ($t_{0.025}(680)$=1.96).

Time series plot of the standardized residuals in Fig. 5a does not show any increasing or decreasing pattern. The ACF of these residuals (Fig. 5b) indicates no apparent departure from the model assumptions as w_t in equation 4.1 being a white noise random variable. The Ljung-Box-Pierce test statistic was found significant at lags H=1 through H=20 (Fig. 5c). The

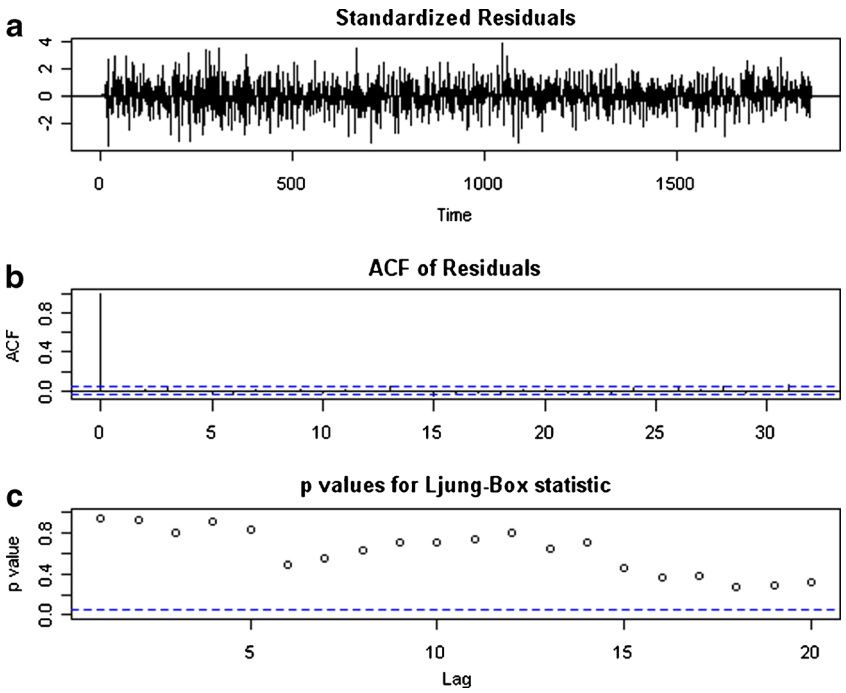

Fig. 5 **a** Time series plot of the standardized residuals. **b** Sample autocorrelation function of the standardized residuals. The *dashed lines* shown on plot b indicate the interval $\pm\frac{1.96}{\sqrt{n}}$ for a white noise sequence; approximately, 95 % of the sample ACFs should be within these limits. **c** The p values for Ljung-Box test at different lags. The *dashed line* shown on c plot indicates $\frac{1.96}{\sqrt{n}}$

significant p value of the Kolmogorov-Smirnov normality test suggests that the residuals are normally distributed. Overall, according to the given information in Fig. 5, the proposed ARIMA model is adequately fitted.

Model verification

To verify the forecasting capability of the developed model, the PGSST anomalies were predicted from January 2007 to June 2011 as an independent test. For instance, when the lead time is 1 month, the SST anomaly of January 2007 was firstly predicted. After this, a new ARIMA model with the period of January 1950 to January 2007 was developed to predict the PGSST anomaly for February 2007. This procedure was sequentially repeated 54 times to predict the PGSST anomalies from January 2007 to June 2011. Similar data prediction was also performed for the lead times of 2 and 3 months. For instance, if the last observed SST data is for February of a year, the model with lead time 1, 2, and 3 months will predict the anomalies data of months March; March and April; and March, April, and May of that particular year, respectively.

Figure 6 illustrates concurrent variations of the observed and predicted PGSST anomalies for the period January 2007 to June 2011 with 1 month lead time. Upper and lower bounds of the 95 % confidence interval of the predicted values are also depicted. As indicated, the applied ARIMA model has recognized the upward trend in the historical data so that all predicted values lie within their 95 % confidence interval. The Pearson correlation coefficient between observed and predicted PGSST anomalies at lead time 1, 2 and 3 months were, respectively, 0.72, 0.69, and 0.65, all statistically significant at 95 % level. The corresponding root mean square errors were 0.33, 0.35, and 0.37 °C.

A 3×3 contingency table was constructed to evaluate the forecast skill of the model (Table not shown). For this evaluation, we characterized cold events as those months for which the observed or predicted SST values are less than the $\bar{x}$−stdev . Likewise, those values for which the SST anomalies were greater than $\bar{x}$−stdev were categorized as the warm incidents. Normal condition was considered as those periods for which the SST anomalies were between these two ranges. The cold, neutral, and warm events were counted in both observed and predicted series, and the results were put in contingency table.

Table 1 Contingency table for the verification of the predicted PGSST anomalies

Obs\Pred (model)	Normal	Warm	Obs
Normal	22	3	25
Warm	8	21	29
Pred	30	24	n=54

Due to the fact that the SST is rapidly increasing in the recent years, no cold event was found in either observed or predicted data. A collapsed form of the 3×3 table which is a 2×2 contingency table was, therefore, used for further analysis (Table 1). The given results suggest that hit rate or the ratio of correct forecast to the total number of cases is 43/54, indicating 79 % the predictions are correct. The hit rate was 75 and 72 % for the 2 and 3 months lead time predictions, respectively. Furthermore, for 1 month lead time, the Heidke's forecast score (Wilks 2011) was found to be 0.59 that is compatible with the results reported by Haklander and Delden (2003) and by Bloomfield et al. (2012). According to these statistics, the developed ARIMA model improved the prediction skill by 59 % as compared with random forecast. The reference accuracy measure in the Heidke score is the correct proportion that would be achieved by random forecasts that are statistically independent of the observations (Wilks 2011). The Heidke's forecast score was found to be 52 or 48 % for 2 or 3 months lead times, respectively.

Detecting the climate change signals

The estimated slope of the Persian Gulf SST $\left(\widehat{\beta}_1\right)$ for the period 1950–2010 was equal to 7.9×10^{-4}°C/month with

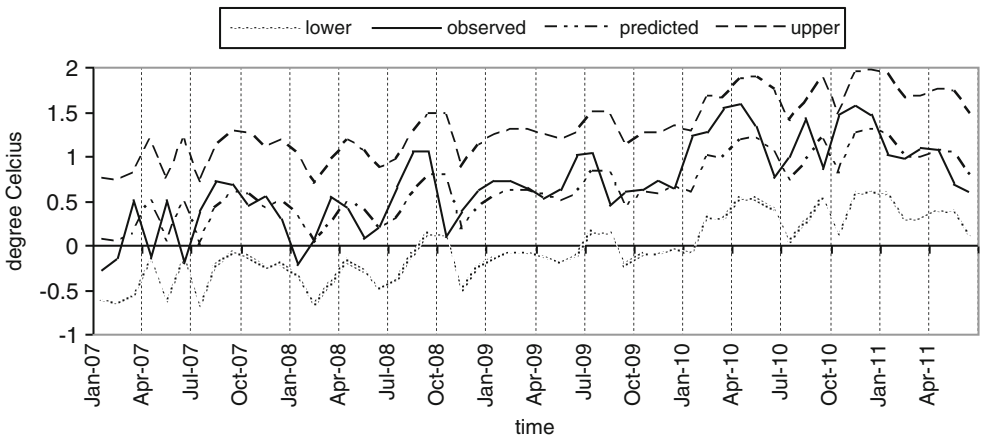

Fig. 6 Concurrent variations of the observed and predicted PGSST anomalies for 1 month lead time. The upper and lower bounds of the predicted values are depicted by the *dashed lines*

standard error of 8.1×10^{-5}°C/month (Fig. 7d). The corresponding t statistic proved the existence of a significant increasing trend in the SST anomalies for this period. The PGSST has, therefore, warmed up by about 0.57 °C during

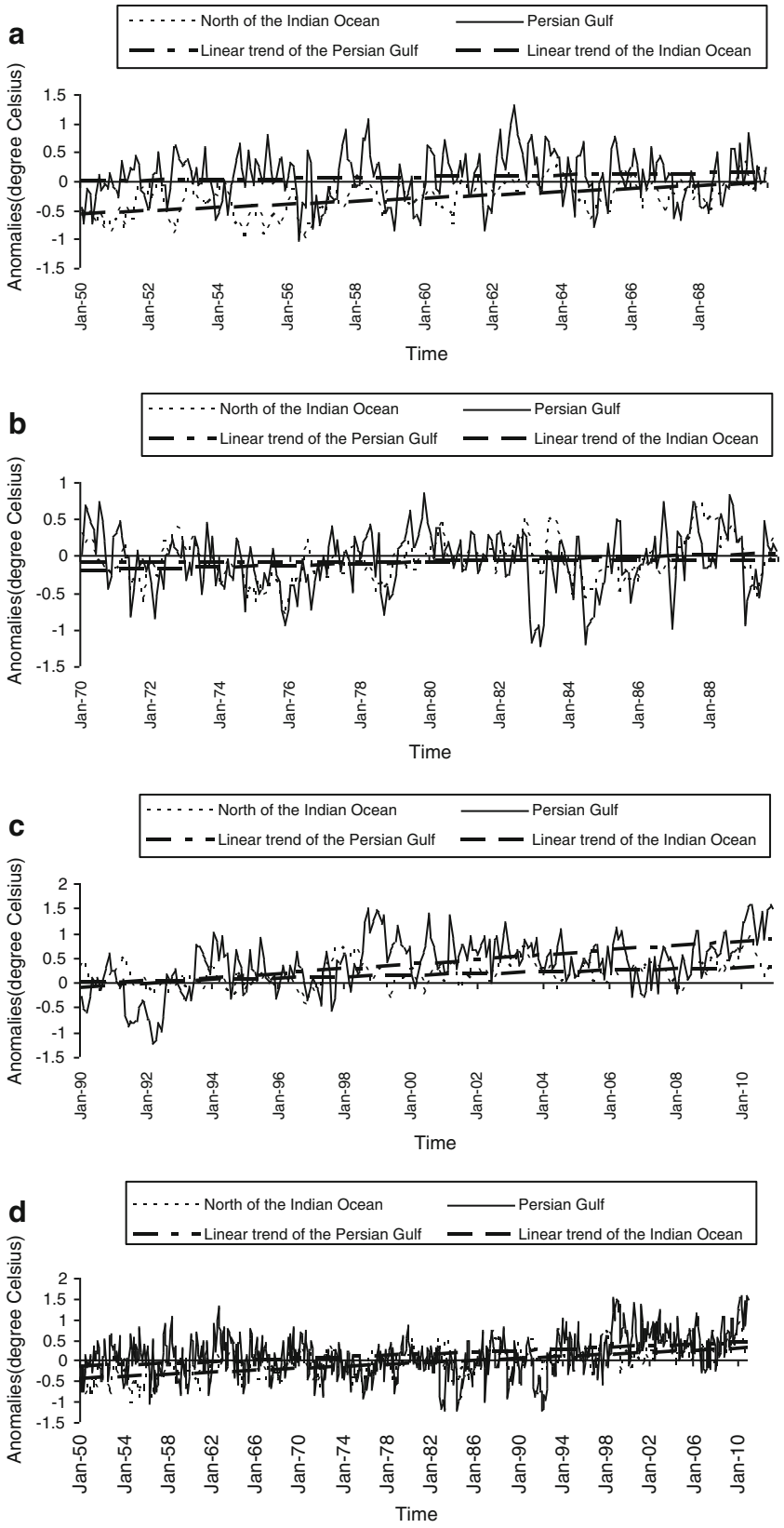

Fig. 7 Time series and trend line plots of the PGSST and north Indian Ocean SST anomalies for the **a** 1950–1969, **b** 1970–1989, **c** 1990, 2010, and **d** 1950–2010 periods

this period. The estimated slopes $\left(\widehat{\beta}_1\right)$ for the period 1950–1969 and 1970–1989 were equal to 5.9×10^{-4}°C/month and 1.3×10^{-4}°C/month indicating the existence of insignificant upward trends (Fig. 7a, b). The slope, however, increased to 3.9×10^{-3}°C/month for the period of 1990–2010, which is strongly significant (Fig. 7c). According to the observational records, the mean PGSSTs for these three periods are 26.57, 26.44, and 26.90 °C, which implicate a slight cooling event over the Gulf during 1960–1989 and an abrupt warming trend for the recent period. This upward trend is about 6.5 times greater than the corresponding values for the period of 1950–1969, suggesting serious threats for the Gulf's ecosystem and biodiversity (Baker-Austin et al. 2012).

Table 2 delineates the trend line slope for southern and northern parts of the Persian Gulf. As indicated, the slope is very smooth and insignificant for the period 1970–1989 for both areas. An abrupt upward trend is, however, evident for both sides and particularly northern areas of the Gulf for the period 1990–2010. While the ratio between the slopes of the recent period to the period 1970–1989 is about 15 for southern side, it is about 102 for northern parts of the Gulf. In contrast to the recent two decades, for both periods of 1950–1969 or 1970–1989, the warming trend in northern side were significantly less than corresponding slopes of southern region. The sudden and threatening warming trend over the northern side of the Gulf needs further explanation.

The obtained Indian Ocean SSTs also exhibited upward trends for all of the 1950–1969, 1970–1989, 1990–2010, and 1950–2010 periods. The slope of the obtained trend lines were, respectively, estimated as 2.2×10^{-3}°C/month, 9.6×10^{-4}°C/month, 1.2×10^{-3}°C/month, and 1×10^{-3}°C/month indicating a consistent and significant upward trend of these SSTs during last six decades (Fig. 7a–d). With the exception of the period 1990–2010, the Indian Ocean's upward trend is astonishingly greater than the corresponding values for the Persian Gulf which is surrounded by arid areas in Iran, Iraq, and the Arabian Peninsula. According to the given statistics, warming trends over the Indian Ocean tropics were about three and seven times more than corresponding values for the Persian Gulf during the period 1950–1969 and 1970–1989, respectively. These ratios, however, dropped to about 0.3 for the 1990–2010 era implicating a sudden and very sharp upward trend for the Gulf SSTs during the last two decades.

Table 2 The slope of the PGSST's linear trends for southern and northern parts of the Gulf

Period\Parts	Southern	Northern
1950–1969	0.00108[a]	0.00012
1970–1989	0.00023	0.00004
1990–2010	0.00349[a]	0.00411[a]
1950–2010	0.00085[a]	0.00073[a]

[a] Significant slope at 5 % level

While both of the Persian Gulf and Indian Ocean SSTs have experienced their lowest warming trend during the period 1970–1989, the highest upward trend over these water bodies occurred during the periods of 1990–2010 and 1950–1969, respectively. In other words, in contrast to the Persian Gulf, the highest warming trend over the considered oceanic areas is related to six to four decades ago. While the ratio between the highest and lowest slopes is about 2.3 for the oceanic area, this ratio reached to 30 for the Persian Gulf region implicating an unexpected jump of this slope over this water body during the 1990–2010 period. Such a sharp warming trend over the Persian Gulf is, therefore, not consistent with either previous SST trend over this water body or corresponding trend over the considered Ocean waters.

Conclusions

Prediction of the Persian Gulf SST anomalies by developing ARIMA models and investigating the signatures of climate change on these SST dataset were two main concerns of the present study. Ground-based and satellite-based SST datasets (ERSST.v3 and OISST, respectively) were applied to examine the reliability of the applied data and the effect of data acquisition methods on the model characteristics. In addition to the Persian Gulf region, the corresponding SST data over northwestern parts of the Indian Ocean tropics were also analyzed. This analysis was conducted to differentiate the natural and anthropogenic sources of climate change over the Persian Gulf. After examining various criteria and thresholds, an elegant ARIMA model, characterized as ARIMA(1,1,2), was developed to predict monthly, two monthly, and three monthly values of the PGSST anomalies. The SST anomalies associated to the ERSST.v3 database was generally found to be greater than corresponding values related to the OISST dataset. Although the model structure was identical when either ERSST.v3 or OISST datasets was used, the model coefficients were found to be dependent on these data sources.

According to the given results, the developed ARIMA model has the hit rate of about 79 % for 1 month lead time suggesting that only 21 % of the predicted events are statistically different with observed events. The hit rate was found to be 75 and 72 % for 2 and 3 months lead times. Furthermore, the Heidke's forecast skill score for 1 month lead time was about 0.59. This suggests that, compared to random prediction, the model improved the prediction accuracy by about 60 % which is a reasonable forecast skill. For two or three monthly prediction, this forecast skill was estimated as 52 and 48 %, respectively. A significant upward trend was detected in the monthly data of the PGSST for the period 1950–2010. Although the trend was not significant for either 1950–1969 or 1970–1990 periods, a sharp increase rate was found for the 1990–2010 period. The observed recent warming trend that is

6.5 greater than corresponding values during 1950–1969 threatens the ecosystem, natural resources, and biodiversity of this water body. It was found that for both of the 1950–1969 and 1970–1989 periods, the SST fluctuations over the southern parts of the Gulf had steeper warming trend as compared with northern areas. Northern regions, however, experienced a sharper increasing temperature trend during 1990–2011 as compared with southern parts. It was shown that the Indian Ocean SSTs have also experienced a significant steady warming trend during the last six decades. With the exception of the recent two decades, the increasing trend over the Persian Gulf was lower than the corresponding trend for the Indian Ocean.

Acknowledgments The authors would like to thank Thomas M. Smith for his valuable suggestions.

References

Akaike H (1974) Markovian representation of stochastic processes and its application to the analysis of autoregressive moving average processes. Ann Inst Stat Math 26:363–387

Baker-Austin C, Trinanes JA, Taylor NGH, Hartnell R, Siitonen A, Martinez-Urtaza J (2012) Emerging Vibrio risk at high latitudes in response to ocean warming. Nat Clim Chang. doi:10.1038/nclimate1628

Barnston AG, Ropelewiski CF (1992) Prediction of ENSO episodes using canonical correlation analysis. J Clim 5:1316–1345

Bauman AG, Pratchett MS, Baird AH, Riegl B, Heron SF, Feary DA (2012) Variation in the size structure of corals is related to environmental extremes in the Persian Gulf. Mar Environ Res. doi:10.1016/j.marenvres.2012.11.007

Bloomfield DS, Higgins PA, McAteer RTJ, Gallagher PT (2012) Toward reliable benchmarking of solar flare forecasting methods, The Astrophysical Journal Letters, 747(2), doi:10.1088/2041-8205/747/2/L41

Box GEP, Pierce DA (1970) Distributions of residuals autocorrelations in autoregressive integrated moving average time series models. J Am Stat Assoc 59:1509–1525

Box GEP, Jenkins GM (1976) Time Series Analysis: Forecasting and Control. San Francisco: Holden-Day

Box GEP, Jenkins GM, Reinsel GC (1994) Time Series Analysis: Forecasting and Control, 3rd edn. Prentice Hall, Englewood Cliffs

Chu PS, Kats RW (1987) Measures of predictability with applications to the Southern Oscillation. Mon Weather Rev 115(8):1542–1549

Chu PS, Kats RW (1985) Modeling of forecasting the Southern Oscillation: a time domain approach. Mon Weather Rev 113:1876–1888

Copsey D, Sutton R, Knight JR (2006) Recent trends in sea level pressure in the Indian Ocean region. Geophys Res Lett 33(19):L19712

Haklander AJ, van Delden A (2003) Thunderstorm predictors and their forecast skill for the Netherlands. Atmos Res 67–68:273–299

Johns W E, Yao F, Olson DB, Josey SA, Grist JP, Smeed DA (2003) Observations of seasonal exchange through the straits of Hormuz and the inferred heat and freshwater budgets of the Persian Gulf. Journal of Geophysical Research: Oceans (1978–2012), 108(C12)

Kämpf J, Sadrinasab M (2006) The circulation of the Persian Gulf: a numerical study. Ocean Sci 2:27–41

Krishnamurti TN, Chakraborty A, Krishnamurti R, Dewar WK, Clayson CA (2006) Seasonal prediction of sea surface temperature anomalies using a suite of 13 coupled atmosphere–ocean models. J Clim 19:6069–6088

Landman WA, Mason SJ (2001) Forecasts of near-global sea surface temperature using canonical correlation analysis. Am Meteorol Soc 15:3819–3833

Ljung GM, Box GEP (1987) On a measure of lack of fit in time series models. Biometrika 65:297–303

Martin M, et al. (2012) Group for high resolution sea surface temperature (GHRSST) analysis fields inter-comparisons: Part 1. A GHRSST multi-product ensemble (GMPE). Deep Sea Research Part II: Topical Studies in Oceanography 77-80: 21–30

Martinez SA, Hsieh WW (2009) Forecasts of tropical Pacific sea surface temperatures by neural networks and support vector regression. Int J Oceanogr 2009:1–13

Mazaris AD, Kornaraki E, Matsinos YG, Margaritoulis D (2004) Modeling the effect of sea surface temperature on sea turtle nesting activities by investigating seasonal trends. Nat Resour Model 17:445–465

Nazemosadat SMJ (1998) The Persian Gulf sea surface temperature as a drought diagnostic for southern parts of Iran. Drought News Netw 10:12–14

Nazemosadat SMJ, Samani N, Barry DA, Molaii Nikoo M (2006) ENSO forcing on climate change in Iran: precipitation analysis. Iran J Sci Technol 30(B4):555–565

Nazemosadat SMJ, Shirvani A (2006) The application of canonical correlation analysis for investigating the influence of Persian Gulf SSTs on winter rainfall of southern Iran. J Agr Sci 29(2):65–77 (in Persian)

Nazemosadat SMJ, Ghasemi AR, Amin SA, Soltani AR (2008) The simultaneous impacts of ENSO and the Persian Gulf SST on the occurrence of drought and wet periods in northwestern Iran, Tabriz University. J Agr Sci 18(3):1–17, in Persian

Neelin JD (1990) A hybrid coupled general circulation model for El-Niño studies. J Agr Sci 47:674–693

Penland C, Magorain P (1993) Prediction of Niño 3 sea surface temperature using linear inverse modeling. Am Meteorol Soc 6:1067–1076

Penland C, Matrosova L (1999) Forecast of tropical Atlantic sea surface temperature using linear inverse modeling. J Clim 11:483–496

Reynolds RW, Smith TM, Liu C, Chelton DB, Casey KS, Schlax MG (2007) Daily high-resolution blended analyses for sea surface temperature. J Clim 20:5473–5496

Shumway RH, Stoffer DS (2006) Time series analysis and its applications with R examples. Springer Science and Business Media, LLC

Smith TM, Reynolds RW, Peterson TC, Lawrimore J (2008) Improvements to NOAA's historical merged land-ocean surface temperature analysis (1880-2006). J Clim 21:2283–2296

Sugiura N (1987) Further analysis of the data by Akaike's information criterion and the finite corrections. Comm Stat Theor Meth 7:13–26

Syu HH, Neelin JD, Gutzler D (1995) Seasonal and interannual variability in a hybrid coupled GCM. J Clim 8:2121–2143

Wilks DS (2011) Statistical methods in the atmospheric sciences, 3rd edn. Academic, San Diego

Xue Y, Leetmaa A, Ji M (2000) ENSO prediction with Markov models: the impact of sea level. J Clim 13:849–871

Xue Y, Smith TM, Reynolds RW (2003) Interdecadal changes of 30-yr SST normals during 1871–2000. J Clim 16:1601–1612

Yao F, Johns WE (2010) A HYCOM modeling study of the Persian Gulf: 2. Formation and export of Persian Gulf Water. J Geophys Res 115(C11):C11017